International Journal of Nanomedicine

Dovepress
open access to scientific and medical research

Open Access Full Text Article

ORIGINAL RESEARCH

Reversal of multidrug resistance by cisplatin-loaded magnetic Fe_3O_4 nanoparticles in A549/DDP lung cancer cells in vitro and in vivo

This article was published in the following Dove Press journal:
International Journal of Nanomedicine
8 May 2013
Number of times this article has been viewed

Ke Li[1]
Baoan Chen[1,2]
Lin Xu[3]
Jifeng Feng[3]
Guohua Xia[1,2]
Jian Cheng[1,2]
Jun Wang[1,2]
Feng Gao[1,2]
Xuemei Wang[4]

[1]Department of Hematology, Key Medical Disciplines of Jiangsu Province, Zhongda Hospital, Medical School, Southeast University, Nanjing, [2]Faculty of Oncology, Medical School, Southeast University, Nanjing, [3]Department of Thoracic Surgery, Jiangsu Province Cancer Hospital, Jiangsu Province, [4]State Key Laboratory of Bioelectronics, Southeast University, Nanjing, People's Republic of China

Abstract: The purpose of this study was to explore whether magnetic Fe_3O_4 nanoparticles (Fe_3O_4-MNP) loaded with cisplatin (Fe_3O_4-MNP-DDP) can reverse DDP resistance in lung cancer cells and to investigate mechanisms of multidrug resistance in vitro and in vivo. MTT assay showed that DDP inhibited both A549 cells and DDP-resistant A549 cells in a time-dependent and dose-dependent manner, and that this inhibition was enhanced by Fe_3O_4-MNP. An increased rate of apoptosis was detected in the Fe_3O_4-MNP-DDP group compared with a control group and the Fe_3O_4-MNP group by flow cytometry, and typical morphologic features of apoptosis were confirmed by confocal microscopy. Accumulation of intracellular DDP in the Fe_3O_4-MNP-DDP group was greater than that in the DDP group by inductively coupled plasma mass spectrometry. Further, lower levels of multidrug resistance-associated protein-1, lung resistance-related protein, Akt, and Bad, and higher levels of caspase-3 genes and proteins, were demonstrated by reverse transcriptase polymerase chain reaction and Western blotting in the presence of Fe_3O_4-MNP-DDP. We also demonstrated that Fe_3O_4-MNP enhanced the effect of DDP on tumor growth in BALB/c nude mice bearing DDP-resistant human A549 xenografts by decreasing localization of lung resistance-related protein and Ki-67 immunoreactivity in cells. There were no apparent signs of toxicity in the animals. Overall, these findings suggest potential clinical application of Fe_3O_4-MNP-DDP to increase cytotoxicity in lung tumor xenografts.

Keywords: Fe_3O_4, nanoparticles, multidrug resistance, reversal, DDP-resistant A549 cells, cisplatin

Introduction

The incidence of lung cancer is increasing worldwide, and non-small cell lung cancer (NSCLC) poses a serious threat to human life and health.[1] Unfortunately, more than half of patients with NSCLC have advanced disease at diagnosis, and have missed the opportunity for surgery, so chemotherapy plays an important role in treatment of the disease. Cisplatin (DDP)-based combination chemotherapies are used as standard treatment for patients with advanced NSCLC and good performance status,[2] and have been shown to achieve significant improvement in overall survival and quality of life.[3,4] However, DDP-based regimens often have severe side effects, which are a frequent cause of poor tolerability, limited therapeutic efficacy, and drug discontinuation.[5] Therefore, novel strategies for treatment of lung cancer are urgently needed.

Recently, one promising strategy to reduce the toxicity of chemotherapy while maintaining its therapeutic effects has been to use drug-coated polymer nanospheres or nanoparticles, which can increase the chemosensitivity of tumor cells.[6,7] Previous studies have shown that magnetic Fe_3O_4 nanoparticles (Fe_3O_4-MNP) when used as

Correspondence: Baoan Chen
Department of Hematology, Zhongda Hospital, Medical School, Southeast University, Nanjing, 210009, People's Republic of China
Tel +86 25 8327 2006
Fax +86 25 8327 2011
Email cba8888@hotmail.com

a drug delivery system can enhance the sensitivity of anticancer drugs and reverse drug resistance in DDP-resistant SKOV3 human ovarian cancer cells.[8,9] Moreover, an in vivo study has shown that Fe_3O_4 nanoparticles copolymerized with daunorubicin and 5-bromotetrandrine strongly inhibit growth of xenograft tumors in nude mice.[10] However, to date, the signal transduction pathways involved in the beneficial effects of Fe_3O_4-MNP in the treatment of lung cancer are largely unknown.

Preclinical research on resistance markers is focused on established human cancer cell lines selected for resistance or on xenografts derived from these cell lines. Multidrug resistance, either inherent or acquired, is a serious problem and one of the most important obstacles to successful treatment of lung cancer. Therefore, a better understanding of drug resistance mechanisms and ways to disrupt the relevant signaling might be an efficient strategy to improve survival of patients with lung cancer.[11] In the past decade, a number of studies of intrinsic resistance of tumor cells to chemotherapy have focused on transporter proteins, including P-glycoprotein, multidrug resistance-associated protein (MRP), and lung resistance-related protein (LRP),[12] which promote resistance by increasing drug efflux, decreasing drug influx, drug inactivation, and alteration of drug targets.[13]

Patient-derived tumor xenografts may also play a key role in the search for more reliable multidrug resistance markers. There is accumulating evidence that several chemotherapeutic agents involved in the treatment of cancer interfere with the phosphatidylinositol 3-kinase/Akt pathway,[14] in which abnormalities of the signal transduction pathway are important in tumorigenesis and tumor progression. Akt is a cytosolic intracellular signal transduction protein that may be a prognostic factor by being closely associated with the development and progression of NSCLC.[15] Further, Ki-67 is a nuclear protein of unclear function, but is present in all proliferating cells, including those in normal and tumor tissue.[16] It is present during all active phases of the cell cycle (G1, S, G2, and mitosis) and is a biologic tumor marker that follows changes in tumor proliferation between pretreated and treated samples, typically core biopsies and surgical samples.[17] Therefore, downregulation of Ki-67 may also be used as a marker of the effect of Fe_3O_4-MNP loaded with DDP (Fe_3O_4-MNP-DDP) on NSCLC xenografts.

Motivated by those considerations, the present study investigated a novel therapeutic strategy targeting DDP-resistant lung cancer in vitro and in vivo, and provides theoretical evidence for its clinical application.

Materials and methods

Materials

The following materials were obtained for use in this study: 3-(4,5-dimethylthiazol-2-yl)-2,5-diphenyltetrazolium bromide (MTT, Sigma, St Louis, MO, USA); cisplatin (Qilu Pharmaceutical Co, Ltd, Jinan, People's Republic of China); RPMI-1640 medium (Gibco BRL, Grand Island, NY, USA); fetal bovine serum (Gibco, Carlsbad, CA, USA); penicillin and streptomycin (Gibco BRL); an Annexin V-fluorescein isothiocyanate (FITC) apoptosis detection kit (Becton Dickinson, Franklin Lakes, NJ, USA); fluorechrome dye 4, 6-diamidino-2-phenylindole (DAPI, Santa Cruz Biotechnology Inc, Santa Cruz, CA, USA); Lipofectamine™ 2000 (Invitrogen Life Technologies, Carlsbad, CA, USA); a reverse transcriptase polymerase chain reaction (RT-PCR) kit (TaKaRa Biotechnology Co, Ltd, Dalian, People's Republic of China); a bicinchoninic acid protein assay kit (Beijing Com Win Biotech Co, Ltd, Beijing, People's Republic of China); monoclonal antihuman MRP1, LRP, Bad, Akt1, P-Akt1, caspase-3, β-actin antibody, and horseradish peroxidase-labeled immunoglobulin G (Santa Cruz Biotechnology Inc); monoclonal anti-LRP and Ki-67 antibody for immunocytochemistry (Sigma); and secondary antimouse biotinylated antibody (Gibco BRL).

Preparation of drug-loaded nanoparticles

Following on from previous studies,[18] Fe_3O_4-MNP were synthesized by electrochemical deposition under oxidizing conditions, and their morphology was observed by transmission electron microscopy (JEM-2100, JEOL, Tokyo, Japan). Before use, the Fe_3O_4-MNP were well dispersed in RPMI-1640 medium containing 10% (v/v) heat-inactivated fetal bovine serum using ultrasound to obtain a colloidal suspension of Fe_3O_4-MNP. Next, 25 μg/mL Fe_3O_4-MNP was added under mechanical stirring to a final volume of 200 μL containing a certain concentration of DDP (v/v). The time taken to polymerize Fe_3O_4-MNP-DDP at 4°C was 24 hours.[9]

Cell lines

Cisplatin-resistant A549 cells were cultured in RPMI-1640 medium supplemented with 10% fetal bovine serum, 2 μmol/L L-glutamine, 100 U/mL penicillin, and 100 μg/mL streptomycin at 37°C, 95% relative humidity, and 5% CO_2. To maintain their drug resistance, DDP-resistant A549 cells were cultured with 5 μg/mL DDP and then cultured further in DDP-free RPMI-1640 medium for two days before starting the experiment.

Cell proliferation assay

For the cell viability assays, 5×10^4/mL of DDP-resistant A549 cells were incubated with Fe_3O_4-MNP, DDP, or Fe_3O_4-MNP-DDP. Meanwhile, A549 cells were incubated with a series of concentrations of DDP, and cells treated with RPMI-1640 medium alone were used as controls. After incubation for 48 hours, 20 μL of MTT solution (5 mg/mL) was added to each well at 37°C in the dark for at least 4 hours. Formazan crystals were dissolved in 200 μL of dimethyl sulfoxide in each well, and reduction of MTT was quantified by absorbance at a measurement wavelength of 540 nm and a reference wavelength of 630 nm using a plate reader (Bio-Rad Laboratories, Tokyo, Japan). The cell inhibition rate was calculated as $(1 - A_{\text{treated cells}}/A_{\text{control cells}}) \times 100\%$. These experiments were repeated at least three times.

Apoptosis assay by flow cytometry

After treatment for 48 hours as described above, the cells were harvested, stained, and evaluated for apoptosis by flow cytometry according to the manufacturer's protocol. Briefly, 1×10^6 cells were stained with 5 μL of Annexin V-FITC for 20 minutes in the dark, and 10 μL of propidium iodide (5 μg/mL) in 1 × binding buffer was then added to each sample. Next, apoptosis was determined by flow cytometry (FACSCalibur, Becton-Dickinson) using Cell Quest software (BD Biosciences, San Jose, CA, USA).

Immunofluorescence staining and confocal microscopy

Cells were cultured on cover slips, and kept in a 35 mm Petri dish for 16–20 hours before treatment. After being cultured for 48 hours as described earlier, the cells were washed with isotonic phosphate-buffered solution (pH 7.4) and then fixed with 4% paraformaldehyde solution for 20 minutes at 37°C. Next, the cover slips were washed three times with phosphate-buffered solution and stained with 2.5 μg/mL DAPI solution for 10 minutes at room temperature. Finally, the cells were washed twice with phosphate-buffered solution, and morphologic changes in apoptotic tumor cells were observed immediately by confocal microscopy (FluoView® FV1000, Olympus, Tokyo, Japan).

Measurement of intracellular DDP accumulation

Intracellular exchange of DDP was measured by inductively coupled plasma mass spectrometry (ICP-MS, X-7 Series, Thermo Fisher Scientific Inc, Waltham, MA, USA).[19] Briefly, 5×10^4/mL cells were incubated with DDP or Fe_3O_4-MNP-DDP for 48 hours. After incubation, the cells were washed twice with phosphate-buffered solution, and centrifuged at 3000 rpm for 30 minutes. The pellet was then dissolved in 33% nitric acid, and the concentration of DDP was determined by ICP-MS.

Transfection

DDP-resistant A549 human lung cells were cultured as described already.[20] Transfection was done with Lipofectamine 2000 under serum-free conditions according to the manufacturer's recommendations. Briefly, DDP-resistant A549 cells were seeded at a density of 5×10^3 into six-well plates for 24 hours, which grew to 50%–70% confluence by the next day. After washing with phosphate-buffered solution, the DDP-resistant A549 cells were transfected by Lipofectamine 2000 using pEGFP-N1 Vector, as in our recently reported study,[21] then incubated at 37°C in a 5% CO_2 incubator for 48 hours. The cells were then cultured in medium containing Geneticin 800–1000 μg/mL. The transfected clones were used for transplantation in vivo.[22]

Tumor model and treatment

BALB/c mice (aged 4 weeks, mean body weight 20 g) were purchased from the Shanghai National Center for Laboratory Animals and kept in a specific pathogen-free environment where temperature was maintained at 22°C and humidity in the range of 40%–50%. Studies involving these mice were performed in adherence with the Guidelines for the Care and Use of Laboratory Animals of the National Institute of Health.

To assess the effect on tumorigenicity, stable transfected DDP-resistant A549 cells were harvested and the BALB/c mice were subcutaneously inoculated on the left abdominal wall with 1×10^7 cells suspended in 0.2 mL of RPMI-1640 medium, for developing the NSCLC xenograft. When tumor sizes in the nude mice had reached an approximate volume of 200 mm^3, calculated by the following equation:

$$\text{Tumor volume V } (mm^3) = 1/2 \times a \times b^2$$

where a is the longest diameter and b is the shortest diameter, the tumor-bearing mice were randomly allocated to a control group, a Fe_3O_4-MNP group, a DDP group, or a Fe_3O_4-MNP-DDP group (n = 6 per group). Each mouse received an intraperitoneal injection of normal saline (0.2 mL), Fe_3O_4-MNP (22 mg/kg in 0.2 mL of normal saline), DDP

(7.5 mg/kg in 0.2 mL of normal saline), or 22 mg/kg Fe_3O_4-MNP and 7.5 mg/kg DDP in normal saline. Tumor growth was monitored by multispectral acquisition and analysis (CRi Maestro™ system, Cambridge Research and Instrumentation Inc, Woburn, MA, USA) for four weeks. Thereafter, the mice were sacrificed and their tumor xenografts were harvested and processed for histopathologic analysis to determine protein expression.

RT-PCR assay

After treatment for 48 hours as described above, total cellular RNA was extracted using TRIzol reagent, and RT-PCR was performed according to the manufacturer's instructions. Briefly, 1 μg samples of total RNA were used to synthesize cDNA at 30°C for 10 minutes, 42°C for 30 minutes, 99°C for 5 minutes, and 5°C for 5 minutes. The newly synthesized cDNA was then amplified by RT-PCR at 94°C for 5 minutes, 94°C for 45 seconds, 55°C for 45 seconds, and 72°C for one minute for 35 cycles. RT-PCR primers were used for MRP1 (526 base pair [bp]) sense: 5′-TC AAATACCTGCTGTTCGG-3′ and antisense: 5′-TGAAGTCCTGTCCTGATGCCA T-3′; LRP (391 bp) sense: 5′-GTGGTGGTAGGAGATGAGTG-3′ and antisense: 5′-CCA GATGTCCACGAGGAGG-3′; Bad (304 bp) sense: 5′-GCTCTTCCTTTGTTCATCTC C-3′ and antisense: 5′-CATCTGGCTCGGGGTTACTGC-3′; Akt1 (159 bp) sense: 5′-T ACTCTTTCCAGACCCACGAC-3′ and antisense: 5′-GGACTACCTGCACTCGGA G-3′; caspase-3 (459 bp) sense: 5′-TGTCGATGCAGCAAACCT-3′ and antisense: 5′-CATCCAGTCGCTTGTGC-3′; β-actin (270 bp) sense: 5′-CTA CAATGAGCTGCG TGTGGC-3′ and antisense: 5′-CAGGTCCAGACGCAGGATGGC-3′. The PCR products were then separated on 1.5% agarose gel and band intensities were quantified directly on gel photographs by Imager Master VDS image analysis (Amersham Pharmacia Biotech, Piscataway, NJ, USA).

Western blot assay

After incubation for 48 hours as described above, the cells were collected and total protein from each sample was separated in 10% sodium dodecyl sulfate polyacrylamide gel electrophoresis gels using a modified radioimmunoprecipitation assay buffer. The proteins were then transferred to a nitrocellulose membrane (Bio-Rad, Hercules, CA, USA). Western blotting was performed with 1:1500 or 1:1000 dilutions of monoclonal antibodies against either antihuman MRP1, LRP, Bad, Akt1, P-Akt1, caspase-3, or β-actin antibody in 5% nonfat milk, followed by horseradish peroxidase-labeled immunoglobulin G as a secondary antibody (1:2000). The blots were visualized by densitometry scans (ECL system, Amersham Biosciences, Little Chalfont, UK) according to the manufacturer's instructions.

Immunocytochemistry study

Tissue sections 4 μm thick were cut from representative formalin-fixed and paraffin-embedded blocks, deparaffinized in xylene, and rehydrated routinely before staining. Sections were treated with 7% hydrogen peroxide in methanol for 20 minutes, microwaved for 5 minutes in citrate phosphate buffer (pH 6.0), and incubated with 5% milk in distilled water for 45 minutes, with thorough washing in phosphate-buffered solution between steps.

Individual sections were incubated with monoclonal anti-LRP and Ki-67 antibody (working dilution 1:100) at 4°C overnight. After washing, the sections were reincubated with a secondary antimouse biotinylated antibody (1:1000) in a dark room for one hour. Next, stained slides were examined to identify localization of LRP and Ki-67 immunoreactivity within the cells. Cytoplasmic staining was considered to be positive for LRP, and nuclear staining was considered to be positive for Ki-67.[23]

Statistical analysis

The data are presented as the mean and standard deviation. All analyses were performed using the Statistical Package for Social Sciences version 13 (SPSS Inc, Chicago, IL, USA). Differences were evaluated using the Student's *t*-test or analysis of variance. $P < 0.05$ was considered to be statistically significant.

Results

Morphology of magnetic Fe_3O_4 nanoparticles

Transmission electron microscopy indicated that the majority of Fe_3O_4-MNPs were spherical in shape with particle sizes of about 30 nm (Figure 1).

Fe_3O_4-MNPs enhanced inhibition of DDP in cells

When DDP-sensitive and DDP-resistant A549 cells were treated with various concentrations of DDP for 12, 24, and 48 hours, DDP-sensitive A549 cells were more sensitive to treatment with DDP than were DDP-resistant A549 cells (Figure 2). MTT assay showed that inhibition of DDP-resistant A549 cells treated with DDP occurred in a time-dependent and dose-dependent manner, and was significantly increased in

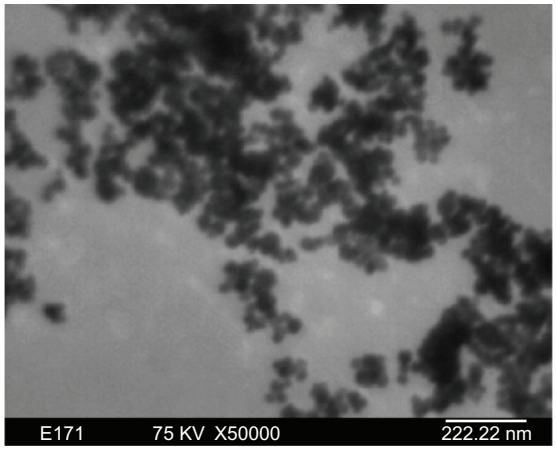

Figure 1 Magnetic Fe_3O_4 nanoparticles seen on transmission electron microscopy.

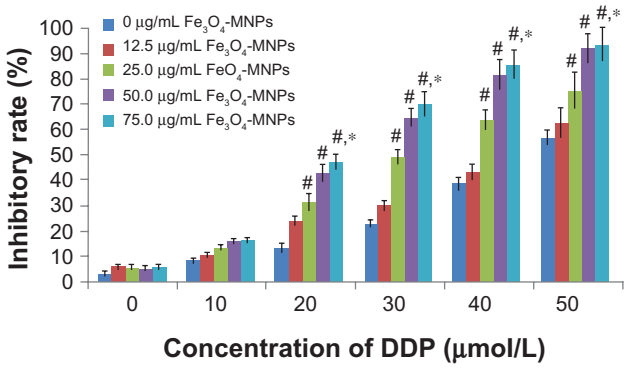

Figure 3 Inhibition of DDP-resistant A549 cells treated with Fe_3O_4-MNP-DDP for 48 hours.
Notes: #$P < 0.05$ versus DDP alone; *$P > 0.05$, no difference between 50.0 μg/mL Fe_3O_4-MNP and 75.0 μg/mL Fe_3O_4-MNP.
Abbreviations: Fe_3O_4-MNP, magnetic Fe_3O_4 nanoparticles; DDP, cisplatin.

the presence of Fe_3O_4-MNP ($P < 0.05$, Figure 3), suggesting that Fe_3O_4-MNP could reverse DDP resistance and enhance cytotoxicity in DDP-resistant A549 cells. Interestingly, Fe_3O_4-MNP alone, at concentrations of 12.5 μg/mL to 75 μg/mL, could slightly inhibit proliferation of DDP-resistant A549 cells, and there was no statistically significant difference compared with the control group ($P > 0.05$, Figure 3), suggesting that Fe_3O_4-MNP did not have marked toxic effects in DDP-resistant A549 cells. On the basis of the findings of our MTT assay and previous research,[9] we selected 25 μg/mL as the optimal concentration of Fe_3O_4-MNP for targeted drug delivery in the present study.

Annexin V-propidium iodide assays for apoptosis

After 48 hours, there was no significant difference in the rate of apoptosis between cells in mice treated with Fe_3O_4-MNP alone and the control group ($P > 0.05$). The apoptotic rate was significantly higher in the group treated with Fe_3O_4-MNP-DDP than in the groups treated with DDP alone or Fe_3O_4-MNP alone, or the control group (Figure 4), suggesting that Fe_3O_4-MNP could enhance DDP-induced apoptosis.

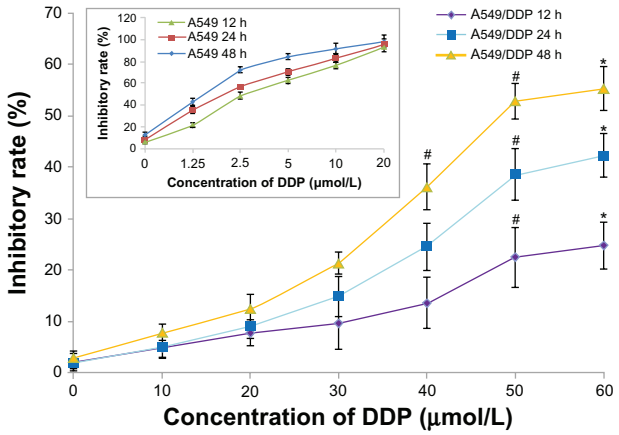

Figure 2 Inhibitory effect of DDP on A549 cells and DDP-resistant A549 cells.
Notes: #$P < 0.05$ versus control group; *$P > 0.05$, no difference between 50 μmol/L DDP and 60 μmol/L DDP at the same time point.
Abbreviation: DDP, cisplatin.

Nuclear morphologic changes in DDP-resistant A549 cells

Nuclear DAPI staining was performed and cells were observed by confocal microscopy to confirm that apoptosis was occurring. DDP-resistant A549 cells in the control and Fe_3O_4-MNP groups were found to have an intact nuclear structure with consistent low-intensity

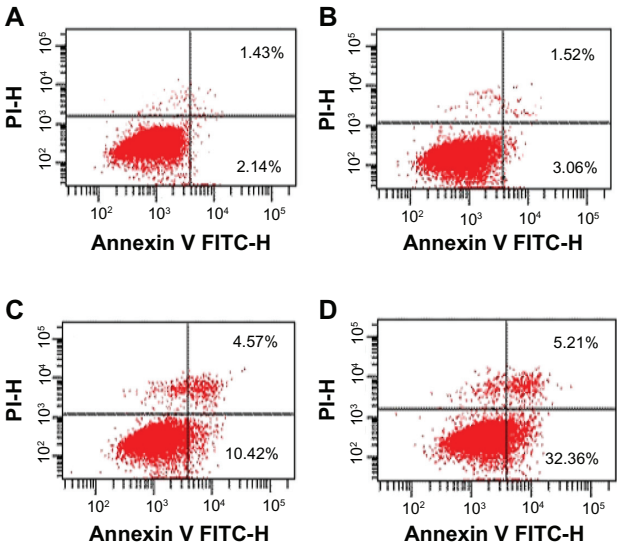

Figure 4 Apoptosis of DDP-resistant A549 cells treated with DDP or Fe_3O_4-MNP-DDP for 48 hours. (**A**) Control, (**B**) 25 μg/mL Fe_3O_4-MNP, (**C**) 20 μmol/L DDP, and (**D**) Fe_3O_4-MNP-DDP.
Abbreviations: Fe_3O_4-MNP, magnetic Fe_3O_4 nanoparticles; DDP, cisplatin; FITC, fluorescein isothiocyanate; PI, propidium iodide.

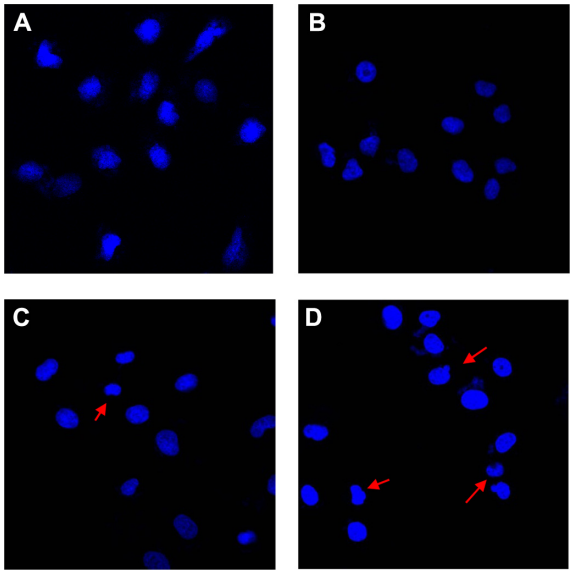

Figure 5 Changes in nuclear morphology of DDP-resistant A549 cells after treatment for 48 hours (DAPI staining, ×400). (**A**) Control, (**B**) 25 μg/mL Fe_3O_4-MNP, (**C**) 20 μmol/L DDP, and (**D**) Fe_3O_4-MNP-DDP.
Notes: The red arrows indicate the apparent apoptotic cells with incomplete nuclear.
Abbreviations: Fe_3O_4-MNP, magnetic Fe_3O_4 nanoparticles; DDP, cisplatin; DAPI, fluorechrome dye 4, 6-diamidino-2-phenylindole.

blue fluorescence (Figure 5A and B), whereas more apparently apoptotic DDP-resistant A549 cells showing high-intensity blue fluorescence were observed in the DDP and Fe_3O_4-MNP-DDP groups (Figure 5C and D). Interestingly, cells in the later stages of apoptosis showing either an irregular cell profile or formation of budding prominences on the cell surface, and apoptotic bodies were subsequently observed more often in the Fe_3O_4-MNP-DDP group (Figure 5D), indicating that Fe_3O_4-MNP could induce apoptosis in DDP-resistant A549 cells exposed to DDD.

Accumulation of intracellular DDP

ICP-MS showed that accumulation of intracellular DDP in the Fe_3O_4-MNP-DDP group was nearly three-fold higher than that in the DDP group (15.28 ± 1.16 μg/L and 5.53 ± 0.09 μg/L, respectively, $P < 0.05$) when DDP-resistant A549 cells had been treated for 48 hours, suggesting that the presence of Fe_3O_4-MNP could prevent drug release from resistant cells and allow marked accumulation of DDP inside DDP-resistant A549 cells.

Transcription of genes by RT-PCR

Computer-assisted image analysis indicated that DDP 20 μmol/L had no obvious effect on the transcription of genes in DDP-resistant A549 cells. Of note, less transcription of MRP1, LRP, Akt1, and Bad as well as higher levels of caspase-3 were detected in the Fe_3O_4-MNP-DDP group than in the control and Fe_3O_4-MNP groups after incubation for 48 hours ($P < 0.05$). However, there were no significant differences in genes detected in DDP-resistant A549 cells between the Fe_3O_4-MNP and control groups ($P > 0.05$, Figure 6).

Protein expression detected by Western blotting

After treatment with Fe_3O_4-MNP-DDP for 48 hours, computer-assisted image analysis showed that levels of MRP1 and LRP proteins were significantly downregulated compared with the control, DDP, and Fe_3O_4-MNP groups ($P < 0.05$), and levels of both proteins were markedly decreased in the presence of Fe_3O_4-MNP (Figure 7). In contrast, there was no significant difference between the Fe_3O_4-MNP and control

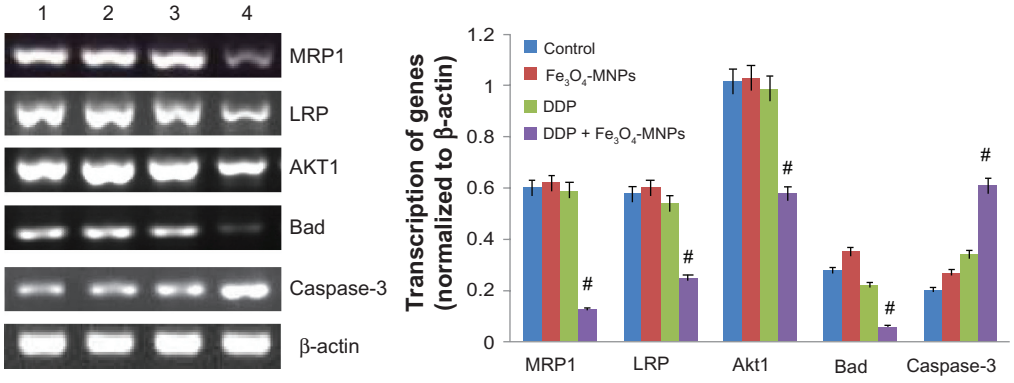

Figure 6 Transcription of mRNA in DDP-resistant A549 cells using reverse transcriptase polymerase chain reaction after treatment for 48 hours.
Notes: Line 1, control; line 2, 25 μg/mL Fe_3O_4-MNP; line 3, 20 μmol/L DDP; line 4, Fe_3O_4-MNP-DDP. $^{\#}P < 0.05$ versus control group.
Abbreviations: Fe_3O_4-MNP, magnetic Fe_3O_4 nanoparticles; DDP, cisplatin; MRP, multidrug resistance-associated protein; LRP, lung resistance-related protein.

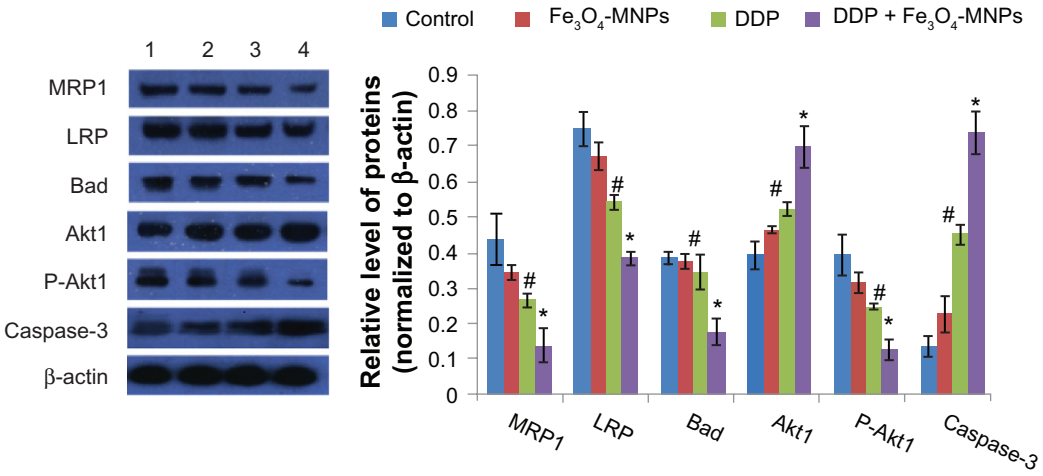

Figure 7 Expression of proteins in DDP-resistant A549 cells after treatment for 48 hours.
Notes: Line 1, control; line 2, 25 μg/mL Fe_3O_4-MNP; line 3, 20 μmol/L DDP; line 4, Fe_3O_4-MNP-DDP. $^{\#}P < 0.05$ versus control group; $^{*}P > 0.05$ versus DDP alone.
Abbreviations: Fe_3O_4-MNP, magnetic Fe_3O_4 nanoparticles; DDP, cisplatin; MRP1, multidrug resistance-associated protein-1; LRP, lung resistance-related protein.

groups ($P > 0.05$), suggesting that Fe_3O_4-MNP can enhance downregulation of LRP and MRP1 expression. We also found that levels of caspase-3 and Akt1 proteins in the DDP group were markedly elevated when compared with levels in the control group ($P < 0.05$), and were enhanced by Fe_3O_4-MNP ($P < 0.05$, Figure 7). In contrast, Akt1 and Bad protein levels in DDP-resistant A549 cells treated with Fe_3O_4-MNP-DDP were lower than those in the control group and in the group treated with DDP alone ($P < 0.05$).

Inhibition of tumor growth

A lump with skin-colored wrinkles was observed in the left abdominal wall of each mouse for approximately a week after injection of the transfected DDP-resistant A549 cells, and tumor volumes soon reached a mean of 200 mm^3. Thereafter, the BALB/c mice were randomly assigned to the treatment groups and were treated for nearly a month, with tumors growing increasingly larger in the Fe_3O_4-MNP and control groups, with no obvious difference between these two groups in tumor volume (554 ± 38 mm^3 and 417 ± 31 mm^3, respectively, $P < 0.05$, Figure 8A and B). Interestingly, tumor volumes in the mice indicated that DDP alone had moderate antitumor efficacy (Figure 8C), whereas subcutaneous tumor growth was suppressed more effectively in mice treated with 22 mg/kg Fe_3O_4-MNP and 7.5 mg/kg DDP (265 ± 23 mm^3 and 149 ± 16 mm^3, Figure 8D), suggesting that the presence of Fe_3O_4-MNP enhanced the effect of DDP on tumor growth.

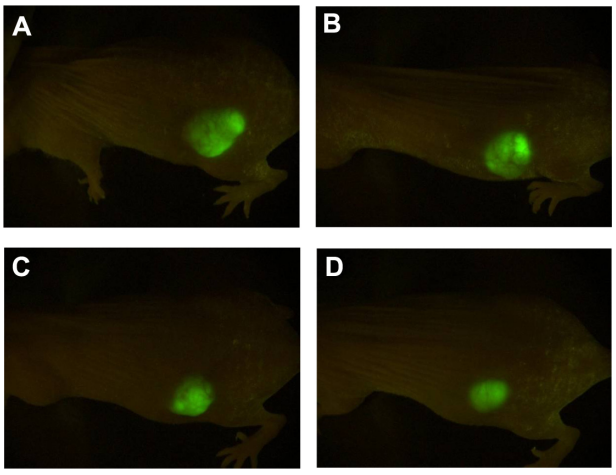

Figure 8 Tumor volumes in mice after treatment for four weeks. (**A**) Control, (**B**) 25 μg/mL Fe_3O_4-MNP, (**C**) 20 μmol/L DDP, and (**D**) Fe_3O_4-MNP-DDP.
Abbreviations: Fe_3O_4-MNP, magnetic Fe_3O_4 nanoparticles; DDP, cisplatin.

Immunocytochemistry

LRP protein was seen to be overexpressed in the cytoplasm of tumor cells from the control and Fe_3O_4-MNP groups (Figure 9A and B), but was markedly decreased after treatment with DDP, with the largest effect seen in the group treated with Fe_3O_4-MNP-DDP (Figure 9C and D). We also found the strongest Ki-67 positivity in the control and Fe_3O_4-MNP groups, with no significant difference in this regard between these two groups (Figure 9E and F). However, expression of Ki-67 was weaker in tissues treated with Fe_3O_4-MNP-DDP (Figure 9G and H).

Toxicity in mice

All of the mice tolerated the study agents satisfactorily, showing no gross signs of cumulative adverse effects, such

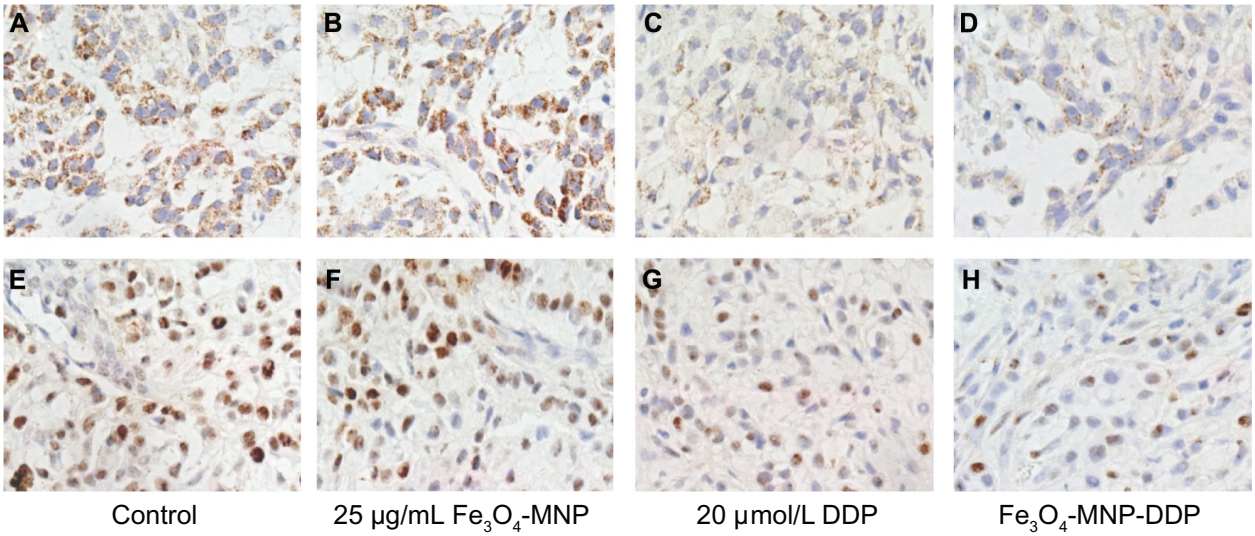

Figure 9 Immunocytochemistry staining for lung resistance-related protein. (**A**–**D**) and Ki-67(**E**–**H**) in mice tumor model tissue (×200).
Abbreviations: Fe_3O_4-MNP, magnetic Fe_3O_4 nanoparticles; DDP, cisplatin.

as weight loss, ruffling of fur, or behavioral and postural changes.

Discussion

Debate continues regarding the value of dose-intense chemotherapy, with analyses suggesting that initially increasing low doses of chemotherapy is of benefit in the treatment of NSCLC, but that little additional benefit is gained using higher doses of chemotherapy.[24] Resistance to cisplatin-based chemotherapy is still one of the major obstacles in the treatment of lung cancer, and is generally considered to be related to multidrug resistance genes, apoptosis-related genes, and abnormal function of DNA repair genes,[25] although the underlying mechanisms are not yet fully understood. To overcome drug resistance and reduce side effects during chemotherapy, a suitable drug delivery system is required to enhance drug accumulation at the tumor site.

During the last few decades, Fe_3O_4-MNP have been the most commonly used magnetic nanoparticles, and are a favorable candidate for directing active anticancer agents to tumors in vivo and to protect sensitive tissues from toxicity.[26] In light of these characteristics, we have focused on their ability to reverse multidrug resistance in lung cancer cells and the mechanisms involved. The Fe_3O_4-MNP prepared for use in this study had a spherical shape and a mean particle size of about 30 nm, and are therefore suitable for biologic application in vitro and in vivo. Our cytotoxicity results show that DDP markedly inhibited growth of A549 cells and DDP-resistant A549 cells in a time-dependent and dose-dependent manner, and that this was augmented by Fe_3O_4-MNP, with no significant effect of Fe_3O_4-MNP alone on DDP-resistant A549 cells (Figures 2 and 3). ICP-MS showed that intracellular DDP concentrations in cells treated with Fe_3O_4-MNP-DDP were higher than those in DDP-treated cells, which may be related to the underlying mechanism for nanoparticles entering cells being endocytotic and/or pinocytotic rather than merely a consequence of simple passive permeation,[27] thus reducing excretion of DDP. This suggests that the presence of Fe_3O_4-MNP can effectively prevent drug release from resistant cells and increase intracellular accumulation of DDP in DDP-resistant A549 cells, which may be related to sustained release of DDP into the cytoplasm and reduced excretion. We also found that rates of apoptosis in DDP-resistant A549 cells were higher in the Fe_3O_4-MNP-DDP group than in the DDP group, which was further demonstrated by the morphologic features of cell nuclei stained with DAPI. All of these observations indicate that Fe_3O_4-MNP can achieve more cytotoxicity and reverse DDP resistance in lung cancer cells via accumulation of DDP inside cells.

Multiple mechanisms are involved in the cytotoxic effects of DDP, and most believe that the multidrug resistance phenomenon is associated with decreased intracellular accumulation of drugs and overexpression of transmembrane transporters, such as P-glycoprotein and MRP1, both of which are members of the ATP-binding cassette protein transporter superfamily, acting as drugs and/or xenobiotic efflux pumps and modifying drug metabolism via glutathione-S-transferase or cytochrome P450 activity, alterations in DNA repair mechanisms, and modifications in apoptotic signaling.[28] MRP, a 190 kDa transmembrane protein, is an ATP-dependent membrane transport protein, and when an

anticancer drug enters a tumor cell, MRP uses the hydrolysis energy of ATP to pump the drug back out of the cell, reducing the intracellular drug concentration and increasing drug resistance.[29] It is generally accepted that increased MRP expression occurs in tumors with multidrug resistance.[30,31] In the present study, we demonstrated that Fe_3O_4-MNP alone could not decrease MRP1 expression, but could enhance downregulation of MRP1 when combined with DDP, which is consistent with observations in other studies.[32] However, some researchers have reported that expression of MRP1 does not occur in response to treatment with cisplatin in lung cancer cell lines or patients,[33] and these conflicting observations might be due to different models being used. On the other hand, LRP, an important part of the vault in human cytoplasm and the nuclear membrane, is also suspected of triggering multidrug resistance and being involved in the intracellular distribution of cytotoxic agents.[34,35] Accumulating evidence indicates that NSCLC with high expression of LRP is resistant to cisplatin.[36,37] In our present study, LRP expression in the Fe_3O_4-MNP-DDP group was less than that in the DDP group, whereas Fe_3O_4-MNP alone did not decrease LRP expression in DDP-resistant A549 cells. These results suggest that the regulatory mechanism of both LRP and MRP1 expression is associated with the multidrug resistance phenotype.[28]

The results of some studies point to the fact that one of the important mechanisms of tumorigenesis and resistance to anticancer drugs is blockade of the pathway triggering apoptosis.[38,39] Understanding of the molecular mechanisms of resistance to DDP may lead to improved treatment strategies for DDP-resistant tumors and increased survival in patients with lung cancer. Recent observations indicate that the phosphatidylinositol 3-kinase and mitogen-activated extracellular signal-regulated kinase pathways may contribute to the effect of Akt activation, which has been shown to be a novel mechanism in promoting resistance to DDP in many human malignances, including lung cancer.[40,41] To ascertain whether the Akt pathway is activated in DDP-resistant A549 cells, we monitored levels of mRNA and protein for Akt1 and observed less transcription and expression of Bad and Akt1; in contrast, we observed higher protein expression of Akt1 in DDP-resistant A549 cells treated with Fe_3O_4-MNP-DDP than in those treated with DDP alone. Moreover, phosphorylation of Akt in DDP-resistant A549 cells decreased after treatment with DDP and inhibition of Akt was markedly enhanced by Fe_3O_4-MNP-DDP. To gain further insight into the mechanism of apoptosis triggered by Fe_3O_4-MNP-DDP, we used a Western blot assay to determine whether activation of caspase-3 was involved in DDP-induced apoptosis in DDP-resistant A549 cells. Our data show that levels of mRNA and protein for caspase-3 in the Fe_3O_4-MNP-DDP group were higher than in controls, including both the Fe_3O_4-MNP and DDP only groups, which further confirms that Fe_3O_4-MNP enhance the effect of DDP on activation of caspase-3. Bad induces apoptosis by inhibiting members of the antiapoptotic Bcl-2 family, such as Bcl-xL, thereby allowing two other proapoptotic members, Bak and Bax, to form complexes, leading to the release of cytochrome c, activation of caspase-3, and apoptosis.[42] In light of the present data and previous findings, the notion that the Akt pathway is involved in cisplatin resistance in lung cancer cell lines is strengthened, and regulation of this pathway may augment apoptosis in DDP-resistant lung cancer cell lines.

It is important to evaluate both the toxicity and potency of any given chemotherapeutic agent in vivo.[43] Patient-derived xenograft models could serve as a link between clinical research and in vitro studies in cell lines. The CRi Maestro is an affordable in vivo system for fluorescence-based small animal imaging and offers improved sensitivity, flexibility, and quantitative accuracy for visible and near-infrared labels. In our present study, multispectral acquisition and analysis showed that tumor volumes in BALB/c mice treated with DDP were moderately decreased in size, whereas those treated with Fe_3O_4-MNP-DDP showed more effective suppression of subcutaneous tumor growth (Figure 8). Interestingly, either injection of a curative dose of DDP or Fe_3O_4-MNP had no obvious side effects on the host within a short period of time based on the body weight of mice. Thus, the use of a Fe_3O_4-MNP formulation is feasible.

On the other hand, preclinical platforms for evaluating novel therapies and prediction markers to monitor standard treatment are required. Immunopositivity for Ki-67 is found in highly proliferative cells, and high Ki-67 immunopositivity is frequently found in poorly differentiated carcinomas.[44,45] Our results showed more nuclear Ki-67 immunoreactivity in tumor model tissues, while those treated with Fe_3O_4-MNP-DDP showed lower nuclear Ki-67 immunoreactivity, indicating that Fe_3O_4-MNP-DDP can inhibit cell proliferation and tumor growth. Further, other researchers have shown that overexpression of LRP in a subgroup of cisplatin-resistant NSCLC cell lines plays an important role in drug resistance, in which involved the NSCLC cells from toxic impacts of cisplatin by intrinsic mechanism.[46] Thus, LRP may be a predictor of the response to treatment in NSCLC. In our present study, high LRP immunoreactivity was observed in the cytoplasm of tumor cells in the control and Fe_3O_4-MNP groups, whereas that in Fe_3O_4-MNP-DDP-treated tumor cells

was clearly decreased, suggesting that Fe_3O_4-MNP-DDP can reverse multidrug resistance and kill tumor cells in vivo. On the basis of the antiproliferative effect of Fe_3O_4-MNP -DDP seen in this study, we postulate that inhibition of growth of solid tumors may also be achievable in vivo.

Conclusion

Overall, the results of this study suggest that Fe_3O_4-MNP enhance the anticancer activity of DDP in vitro and in vivo without obvious systemic toxicity. Therefore, there is the potential for clinical application of Fe_3O_4-MNP-DDP to reverse DDP resistance in lung cancer cells.

Acknowledgments

This work was supported by grants from the National Key Basic Research Program 973 of China (2010CB732404), the National Natural Science Funds of the People's Republic of China (81170492), the Key Medical Disciplines of Jiangsu Province and Nanjing Medical University Science and Technology Development Funds Key Program (2012 NJMU151), and the Science Foundation of Jiangsu Province Cancer Hospital (ZM 200901).

Disclosure

The authors report no conflicts of interest in this work.

References

1. Zhou W, Christiani DC. East meets West: ethnic differences in epidemiology and clinical behaviors of lung cancer between East Asians and Caucasians. *Chin J Cancer*. 2011;30:287–291.
2. Ohe Y, Ohashi Y, Kubota K, et al. Randomized phase III study of cisplatin plus irinotecan versus carboplatin plus paclitaxel, cisplatin plus gemcitabine, and cisplatin plus vinorelbine for advanced non-small-cell lung cancer: Four-Arm Cooperative Study in Japan. *Ann Oncol*. 2007;18:317–323.
3. Tsuboi M, Ohira T, Saji H, et al. The present status of postoperative adjuvant chemotherapy for completely resected non-small cell lung cancer. *Ann Thorac Cardiovasc Surg*. 2007;13:73–77.
4. Pignon JP, Tribodet H, Scagliotti GV, et al. Lung adjuvant cisplatin evaluation: a pooled analysis by the LACE Collaborative Group. *J Clin Oncol*. 2008;26:3552–3559.
5. Rossi A, Maione P, Gridelli C. Safety profile of platinum-based chemotherapy in the treatment of advanced non-small cell lung cancer in elderly patients. *Expert Opin Drug Saf*. 2005;4:1051–1067.
6. Farokhzad OC, Cheng JJ, Teply BA, et al. Targeted nanoparticle-aptamer bioconjugates for cancer chemotherapy in vivo. *Proc Natl Acad Sci U S A*. 2006;103:6315–6320.
7. Perrotta C, Bizzozero L, Falcone S, et al. Nitric oxide boosts chemoimmunotherapy via inhibition of acid sphingomyelinase in a mouse model of melanoma. *Cancer Res*. 2007;67:7559–7564.
8. Xia GH, Chen BA, Ding JH, et al. Effect of magnetic Fe_3O_4 nanoparticles with 2-methoxyestradiol on the cell-cycle progression and apoptosis of myelodysplastic syndrome cells. *Int J Nanomedicine*. 2011;6:1921–1927.
9. Jiang Z, Chen BA, Xia GH, et al. The reversal effect of magnetic Fe_3O_4 nanoparticles loaded with cisplatin on SKOV3/DDP ovarian carcinoma cells. *Int J Nanomedicine*. 2009;4:107–114.
10. Chen BA, Cheng J, Wu NY, et al. Reversal of multidrug resistance by magnetic Fe_3O_4 nanoparticle copolymerizating daunorubicin and 5-bromotetrandrine in xenograft nude-mice. *Int J Nanomedicine*. 2009;4:73–78.
11. Singh A, Boldin-Adamsky S, Thimmulappa RK, et al. RNAi-mediated silencing of nuclear factor erythroid-2-related factor 2 gene expression in non-small cell lung cancer inhibits tumor growth and increases efficacy of chemotherapy. *Cancer Res*. 2008;68:7975–7984.
12. Li J, Li ZN, Yu LC, et al. Association of expression of MRP1, BCRP, LRP and ERCC1 with outcome of patients with locally advanced non-small cell lung cancer who received neoadjuvant chemotherapy. *Lung Cancer*. 2010;69:116–122.
13. Longley DB, Johnston PG. Molecular mechanisms of drug resistance. *J Pathol*. 2005;205:275–292.
14. Schatz JH. Targeting the PI3K/AKT/mTOR pathway in non-Hodgkin's lymphoma: results, biology, and development strategies. *Curr Oncol Rep*. 2011;13:398–406.
15. Oh Y, Herbst RS, Burris H, et al. Enzastaurin, an oral serine/threonine kinase inhibitor, as second- or third-line therapy of non-small-cell lung cancer. *J Clin Oncol*. 2008;26:1135–1141.
16. Urruticoechea A, Smith IE, Dowsett M. Proliferation marker Ki-67 in early breast cancer. *J Clin Oncol*. 2005;23:7212–7220.
17. Torrisi R, Bagnardi V, Cardillo A, et al. Preoperative bevacizumab combined with letrozole and chemotherapy in locally advanced ER- and/or Pg R-positive breast cancer: clinical and biological activity. *Br J Cancer*. 2008;99:1564–1571.
18. Chen BA, Sun Q, Wang XM, et al. Reversal in multidrug resistance by magnetic nanoparticle of Fe_3O_4 loaded with adriamycin and tetrandrine in K562/AO2 leukemic cells. *Int J Nanomedicine*. 2008;3:277–286.
19. Brouwers EEM, Tibben MM, Pluim D, et al. Inductively coupled plasma mass spectrometric analysis of the total amount of platinum in DNA extracts from peripheral blood mononuclear cells and tissue from patients treated with cisplatin. *Anal Bioanal Chem*. 2008;391:577–585.
20. Ma QS, Li P, Xu MY, et al. Ku80 is highly expressed in lung adenocarcinoma and promotes cisplatin resistance. *Exp Clin Cancer Res*. 2012;31:99.
21. Chen BA, Mao PP, Cheng J, et al. Reversal of multidrug resistance by magnetic Fe_3O_4 nanoparticle copolymerizating daunorubicin and MDR-1 shRNA expression vector in leukemia cells. *Int J Nanomedicine*. 2010;5:437–444.
22. Hellweg CE, Baumstark-Khan C, Horneck G. Enhanced green fluorescent protein as reporter protein for biomonitoring of cytotoxic effects in mammalian cells. *Anal Chim Acta*. 2001;427:191–199.
23. Yurdakul A, Akyurek N, Yilmaz S, et al. Prognostic impact of matrix metalloproteinases (MMP-9 and MMP-2) and vascular endothelial growth factor expression in non-small cell lung cancer. *Turk J Med Sci*. 2012;42:281–288.
24. Stewart DJ, Chiritescu G, Dahrouge S, Banerjee S, Tomiak EM. Chemotherapy dose-response relationships in non-small cell lung cancer and implied resistance mechanisms. *Cancer Treat Rev*. 2007;33:101–137.
25. Seve P, Dumontet C. Chemoresistance in non-small cell lung cancer. *Curr Med Chem Anticancer Agents*. 2005;5:73–88.
26. Thomas K, Sayre P. Research strategies for safety evaluation of nanomaterials. Part I: Evaluating the human health implications of exposure to nanoscale materials. *Toxicol Sci*. 2005;87:316–321.
27. Soma CE, Dubernet C, Bentolila D, et al. Reversion of multidrug resistance by co-encapsulation of doxorubicin and cyclosporin A in polyalkyleyanoacrylate nanoparticles. *Biomaterials*. 2000;21:1–7.
28. Bouhamyia L, Chantot-Bastaraud S, Zaidi S, et al. Immunolocalization and cell expression of lung resistance-related protein (LRP) in normal and tumoral human respiratory cells. *J Histochem Cytochem*. 2007;55:773–782.
29. McGrath T, Center MS. Adriamycin resistance in HL60 cells in the absence of detectable P-glycoprotein. *Biochem Biophys Res Commun*. 1987;145:1171–1176.

30. Burger H, Foekens JA, Look MP, et al. RNA expression of breast cancer resistance protein, lung resistance-related protein, multidrug resistance-associated proteins1 and 2, and multidrug resistance gene 1 in breast cancer: correlation with chemotherapeutic response. *Clin Cancer Res*. 2003;9:827–836.
31. Steinbach D, Wittig S, Cario G, et al. The multidrug resistance-associated protein 3 (MRP3) is associated with a poor outcome in childhood ALL and may account for the worse prognosis in male patients and T-cell immunophenotype. *Blood*. 2003;102:4493–4498.
32. Berger W, Elbling L, Hauptmann E, Micksche M. Expression of the multidrug resistance-associated protein (MRP) and chemoresistance of human non-small-cell lung cancer cells. *Int J Cancer*. 1997;73:84–93.
33. Filipits M, Haddad V, Schmid K, et al. Multidrug resistance proteins do not predict benefit of adjuvant chemotherapy in patients with completely resected non-small cell lung cancer: International Adjuvant Lung Cancer Trial Biologic Program. *Clin Cancer Res*. 2007;13:3892–3898.
34. Triller N, Korosec P, Kern I, Kosnik M, Debeljak A. Multidrug resistance in small cell lung cancer: expression of P-glycoprotein, multidrug resistance protein 1 and lung resistance protein in chemo-naive patients and in relapsed disease. *Lung Cancer*. 2006;54:235–240.
35. Scheper RJ, Broxterman HJ, Scheffer GL, et al. Overexpression of a M(r) 110,000 vesicular protein in non-P-glycoprotein-mediated multidrug resistance. *Cancer Res*. 1993;53:1475–1479.
36. van Zon A, Mossink MH, Schoester M, Scheper RJ, Sonneveld P, Wiemer EAC. Efflux kinetics and intracellular distribution of daunorubicin are not affected by major vault protein/lung resistance-related protein (vault) expression. *Cancer Res*. 2004;64:4887–4892.
37. Berger W, Elbling L, Micksche M. Expression of the major vault protein LRP in human non-small-cell lung cancer cells: Activation by short-term exposure to antineoplastic drugs. *Int J Cancer*. 2000;88:293–300.
38. Groeger AM, Esposito V, De Luca A, et al. Prognostic value of immunohistochemical expression of p53, bax, Bcl-2 and Bcl-x (L) in resected non-small-cell lung cancers. *Histopathology*. 2004;44:54–63.
39. Tsuruo T, Naito M, Tomida A, et al. Molecular targeting therapy of cancer: drug resistance, apoptosis and survival signal. *Cancer Sci*. 2003;94:15–21.
40. Yang X, Fraser M, Abedini MR, Bai T, Tsang BK. Regulation of apoptosis-inducing factor-mediated, cisplatin-induced apoptosis by Akt. *Br J Cancer*. 2008;98:803–808.
41. Liu Z, Zhou XD, Qian G, Shi X, Fang J, Jiang BH. AKT1 amplification regulates cisplatin resistance in human lung cancer cells through the mammalian target of rapamycin/p70S6 K1 pathway. *Cancer Res*. 2007;67:6325–6332.
42. Wei MC, Zong WX, Cheng EH, et al. Proapoptotic BAX and BAK: a requisite gateway to mitochondrial dysfunction and death. *Science*. 2001;292:727–730.
43. Cozzi P. The discovery of a new potential anticancer drug: a case history. *Farmaco*. 2003;58:213–220.
44. Ramljak V, Sucic M, Vrdoljak DV, Borojevic N. Expression of Ki-67 and p27 Kip1 in fine-needle aspirates from breast carcinoma and benign breast diseases. *Diagn Cytopathol*. 2011;39:333–340.
45. von Minckwitz G, Sinn HP, Raab G, et al. Clinical response after two cycles compared to HER2, Ki-67, p53, and bcl-2 in independently predicting a pathological complete response after preoperative chemotherapy in patients with operable carcinoma of the breast. *Breast Cancer Res*. 2008;10:R30.
46. Harada T, Ogura S, Yamazaki K, et al. Predictive value of expression of P53, Bcl2 and lung resistance-related protein for response to chemotherapy in non-small cell lung cancers. *Cancer Sci*. 2003;94:394–399.